05

Shock compressibility and spall strength of the composite based on Kevlar and the epoxy resin

© A.V. Utkin, V.M. Mochalova, A.V. Savchenko, V.E. Breykina

Federal Research Center of Physics and Medical Chemistry of Russian Academy of Sciences, 142432, Chernogolovka, Moscow Region, Russia

e-mail: utkin@icp.ac.ru

Received November 7, 2024 Revised March 25, 2025 Accepted March 25, 2025

This paper performed experimental studies of shock-wave properties of a composite of an ballistic aramid fabric and an epoxy binder with longitudinal and transverse orientation of fibers in relation of a wave propagation direction. Profiles of a particle velocity were recorded by means of laser interferometry. It is shown that a shock Hugoniot of the composite does not depend on orientation of the fibers and at 17 GPa it exhibits a break that indicates chemical decomposition. The most pronounced feature of the velocity profiles in the samples with longitudinal orientation of the fibers is a two-wave configuration at the pressure of shock compression below 12 GPa. It is shown that the spall strength of the Kevlar-based composite with longitudinal orientation of the fibers is approximately two times higher than with transverse orientation and is 180 MPa.

Keywords: composite, shock waves, shock Hugoniot, spall strength, Kevlar, epoxy resin.

DOI: 10.61011/TP.2025.07.61452.410-24

Introduction

Fiber-reinforced polymer composites have high temperature and chemical resistance, a low thermal expansion coefficient, and their strength and stiffness per unit weight is higher than that of the most metals. For this reason, they are widely used in various industries as structural elements. These composites are heterogeneous anisotropic materials and their mechanical properties depend not only on the structure, composition and used matrix, but on orientation of the fibers as well.

The papers dedicated to studying low- and high-velocity impact on the composite materials containing various types of the fibers, including carbon, aramid, glass fibers, and superhigh molecular polyethylene [1–21] as well as on their matrix [22–30] have been analyzed to show that there is a pronounced individual reaction of the composites to the pulse impact. The shock-wave methods make it possible to obtain factful information about the properties of the anisotropic heterogeneous materials under extreme loading conditions.

Since these materials are widely used in various structures affected by intense impacts, it is essentially important to study their strength under static and dynamic loads. The experiments under shock-wave impact also include determination of a material strength under pulse tension, i.e. the spall strength. It is not enough to know the component composition and the structure of the heterogeneous anisotropic materials for predicting the strength properties of the composites under various test conditions. Other properties of the materials, such as adhesion between a filler and the matrix may also be essential. It was shown

in the paper [17] with adding only 0.5% of nanotubes into the Kevlar, a fracture start threshold is increased by 30% in comparison with the Kevlar samples. The similar result was observed in the study [18] with shock-wave impact on the Kevlar composites with nanoclay, which contain the epoxy matrix. The spall strength of the epoxy resin and the composites based thereon has been investigated to show that fiber additives usually make no impact on the value of the spall strength of the epoxy resin or substantially reduce it [5,12,19,24,31,32]. It was also shown for some composites that the value of the spall strength of these materials can substantially depend on a direction of propagation of the shock wave in relation of fiber arrangement [12,33]. The heterogeneous structure of the composites results in noticeable complication of dynamics of the wave effects, which does not always make it possible to use traditional methods of estimation of the value of the spall strength. In particular, it is important to take into account possible formation of multiple spallation, which is a known phenomenon and considered, for example, in the studies [34-36]. This nature of fracture was observed by the authors [5] on preserved samples of the Kevlar/epoxy matrix composite as well as in the study [13] when recording motion of the UHMWPE-composite sample by a high-speed camera during shock-wave impact.

In addition to the spall strength, the study of the sample at high pressures makes it possible to obtain information about their impact compressibility, i.e. the shock Hugoniot. Some authors have shown that depending on the structure, arrangement and volume content of the fibers in the material, its Hugoniot could both depend and not depend on the direction of propagation of the shock wave [5,7,10,12,37,38].

For example, for unidirectional carbon fiber-reinforced plastic containing more than 60 weight% of carbon fibers, at the pressure below 10 GPa there is a recorded different behavior of the composite depending on its orientation [7,9,39]. In the unidirectional composite based on the aramid fibers [12], with their content of about 65%, the difference of impact compressibility with longitudinal and transverse orientations of the fibers is observed within the entire range of the studied pressures — approximately up to 35 GPa.

Thus, it is clear from analysis of the studies of the composites and their binders under shock-wave impact that each case exhibits an individually pronounced response of the samples. Therefore, experimental investigation of the composite materials under the pulse impact will make it possible to identify general relationships of their compressibility, strain and fracture. The aim of the present study is to experimentally study the Hugoniot and the spall strength of the composite made of the aramid ballistic fabric (ballistic Kevlar) and the epoxy binder with propagation of the shock wave in a longitudinal and a transverse direction in relation to orientation of the fibers. Relevance and novelty of the study are due to the fact that previously the shock-wave investigations of this composite have not been performed, while there are known experimental data that are obtained for the similar composite with another structure of the aramid fiber [3,5]. Comparison of the results will make it possible to identify specific features of a reaction of the materials similar in composition to the pulse impact.

Structure of the samples made of ballistic Kevlar and epoxy resin. Experimental diagram

The initial samples of the composite were the plates of the size 50×50 mm, of the thickness from 3 to 8 mm, which are made of 11-26 layers of the aramid ballistic fabric of a paraamid fiber (the density of 255 g/m²) and the epoxy binder L+EPH161 (Fig. 1). The density of the aramid fiber is 1.45 g/cm³, the density of the epoxy resin is 1.15 g/cm³. The volume content of the fibers is 50%, and the weight content of the fibers is 55.8%. The plates are made by vacuum infusion. The density of the samples was $1.306 \,\mathrm{g/cm^3}$. Since the composite is anisotropic, the speed of sound depends on the wave propagation direction. It was measured by an ultrasonic technique to obtain the following values of the speed of sound: along the fibers $C_{\parallel} = (5.302 \pm 0.003) \, \text{km/s}$, and in a reverse direction. $C_{\perp} = (2.661 \pm 0.003)$ km/s.

The shock-wave loading was implemented by a collision with aluminum plates, so when using the samples shown in Fig. 1, the shock waves are formed and propagate across the fibers. In order to investigate the impact compressibility along the fibers, the initial plates were cut into strips of the thickness of 8 mm and glued by the epoxy resin so that the fibers were perpendicular to the sample plane.

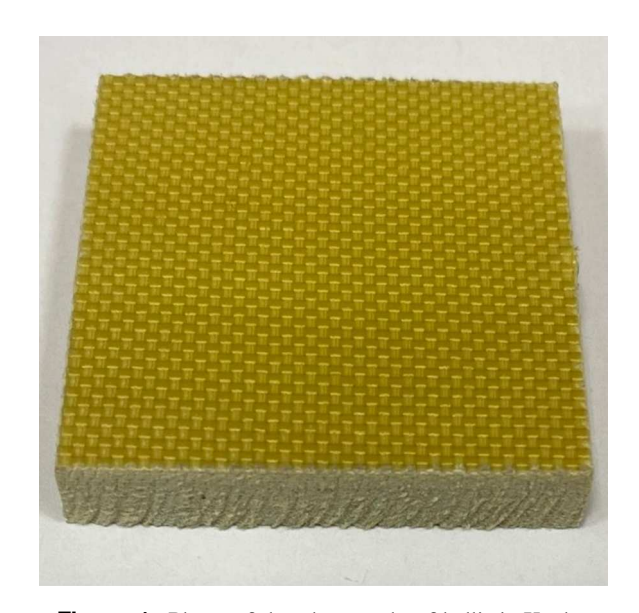


Figure 1. Photo of the plate made of ballistic Kevlar.

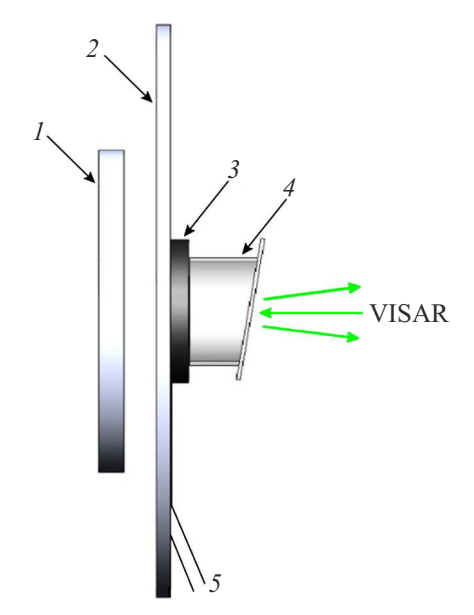


Figure 2. Experimental diagram: I — the aluminum projectile, 2 — the baseplate, 3 — the sample, 4 — the water window, 5 — the polarization gauge.

The diagram of the experimental assembly is shown in Fig. 2. The projectiles I were accelerated by explosion propellant devices. The shock waves in the studied samples 3 were formed by the collision of the aluminum projectile I of the diameter of 90 mm, which is accelerated by explosion products to the velocity W_i , with the baseplate 2. The interferometer VISAR [40] was used to measure the velocity of a sample/water interface 4. Laser radiation was reflected from an aluminum foil of the thickness of 7μ m, which was glued to the sample. In order to determine an absolute value of the velocity, reflected radiation was recorded by two interferometers with velocity fringe constants 280

and $1280\,\mathrm{m/s}$. In each test, the polarization gauge 5 recorded a time of entry of the shock wave into the sample, which made it possible to find the value of the shock wave velocity U_s using the interferometric data. The error of determination of U_s is determined by accuracy of measurement of the sample thickness (that is $\pm 0.01\,\mathrm{mm}$) and by accuracy of recording the time of transmission of the shock wave through the sample, which is defined by equipment characteristics and is $\pm 2\,\mathrm{ns}$. Since the sample thickness exceeded 3 mm, and the recording time was $\sim 1\,\mu\mathrm{s}$, the error of determination of Us was $\pm 0.5\,\%$ $\pm 0.5\,\%$.

The experimental diagram for determining the spall strength is similar to that of Fig. 2, but without the water window, and the interferometer recorded the velocity of a free surface. To maintain uniaxial strain during the entire time of recording of the shock-wave processes [41], the sample thickness was from 3 to 4.5 mm, which is by an order less than their diameter. Then, respectively, the quantity of the aramid fabric in the samples when studying the spall strength was 11-15 layers.

2. Shock-wave compressibility of the polymer based on ballistic Kevlar

The parameters of the experimental assemblies and the results of the experiments for investigating the shockwave compressibility of ballistic Kevlar with transverse and longitudinal orientation of the fibers are given in Table 1 and Fig. 3–7. Table 1 shows the speed of the aluminum projectile W_i and its thickness h_i , the material of the baseplate and its thickness of h_b , the measured shock-wave velocity U_s , the pressure P and the particle velocity u_p . The pressure and the particle velocity were calculated by the

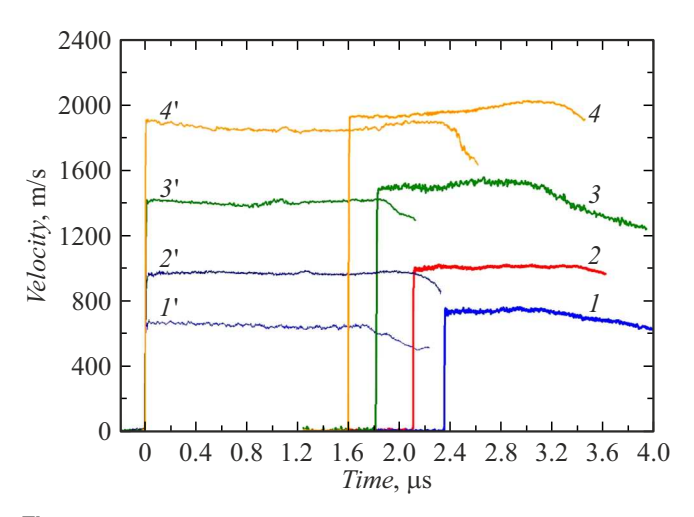


Figure 3. Particle velocity profiles at the composite/water interface with transverse orientation of the fibers and the pressure below 15 GPa.

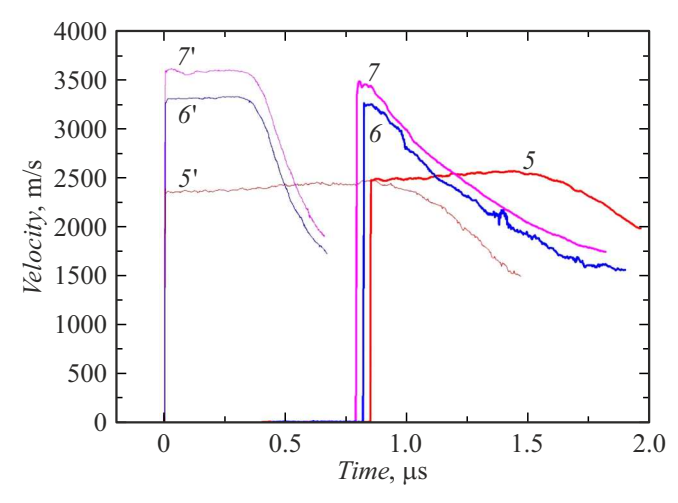


Figure 4. Particle velocity profiles at the composite/water interface with transverse orientation of the fibers and the pressure above 15 GPa.

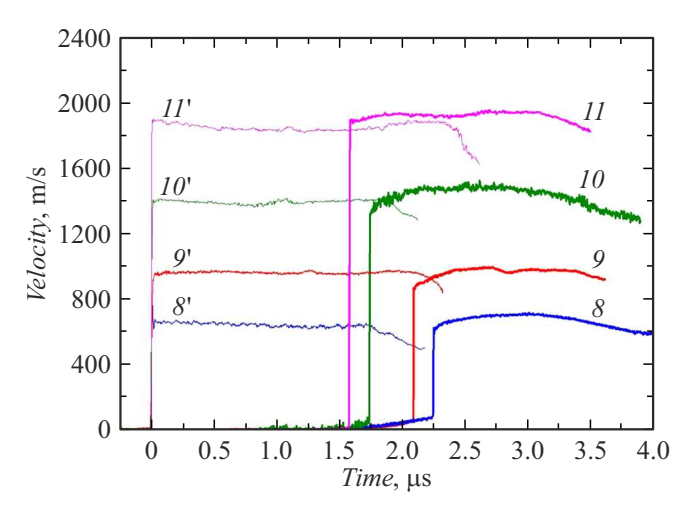


Figure 5. Particle velocity profiles at the sample/water interface with longitudinal orientation of the fibers and the pressure below 15 GPa.

measured values of W_i , U_s and the known shock Hugoniots of the materials of the projectile and the baseplate.

The figures 3 and 4 show the velocity profiles at the sample/water interface with transverse orientation of the fibers in relation to the direction of propagation of the shock wave, while the figures 5 and 6 show the same with longitudinal orientation. The digit designations of the presented dependences coincide with number of the experiments of Table 1. Besides, the thin lines (at $0\,\mu s$) show compression pulses entering the studied samples, which were measured at the baseplate/water interface. They are designated with the same digits (with primes) as the experiments corresponding thereto.

The tests 1-5 and 8-12 used relatively thick aluminum projectiles — from 5 to $10 \, \text{mm}$, so after a shock jump the amplitude of the shock wave entering the sample is still constant during the time from 0.8 to $2.4 \, \mu \text{s}$. In the tests 6,

№	W_i , km/s	h_i , mm	h_b , mm	h_s , mm	U_s , km/s	u_p , km/s	P, GPa	V, cm ³ /g					
Transverse orientation of the fibers													
1	1.13	7	Cu, 5.5	7.90	3.61 ± 0.05	0.60 ± 0.02	2.83 ± 0.05	0.638 ± 0.006					
2	1.13	7	Al, 4.0	7.85	3.93 ± 0.05	0.85 ± 0.02	4.36 ± 0.05	0.600 ± 0.006					
3	2.50	10	Cu, 5.5	7.95	4.70 ± 0.05	1.34 ± 0.02	8.23 ± 0.05	0.547 ± 0.006					
4	2.50	10	Al, 4.0	7.92	5.41 ± 0.05	1.77 ± 0.02	12.51 ± 0.10	0.515 ± 0.006					
5	3.30	5	Al, 4.0	4.43	5.97 ± 0.05	2.30 ± 0.05	17.93 ± 0.15	0.471 ± 0.006					
6	4.60	2	Al, 2.0	4.40	6.48 ± 0.05	3.21 ± 0.05	27.17 ± 0.20	0.386 ± 0.006					
7	5.05	2	Al, 2.0	4.30	6.72 ± 0.05	3.51 ± 0.05	30.80 ± 0.20	0.366 ± 0.006					
Longitudinal orientation of the fibers													
8	1.13	7	Cu, 5.5	7.50	3.59 ± 0.05	0.60 ± 0.02	2.81 ± 0.05	0.638 ± 0.006					
9	1.13	7	Al, 4.0	7.55	3.85 ± 0.05	0.85 ± 0.02	4.27 ± 0.05	0.597 ± 0.006					
10	2.50	10	Cu, 5.5	7.30	4.56 ± 0.05	1.35 ± 0.02	8.04 ± 0.05	0.539 ± 0.006					
11	2.50	10	Al, 4.0	7.56	5.25 ± 0.05	1.78 ± 0.02	12.20 ± 0.1	0.506 ± 0.006					
12	3.30	5	Al, 4.0	4.43	5.91 ± 0.05	2.30 ± 0.05	17.75 ± 0.15	0.468 ± 0.006					
13	4.60	2	Al, 2.0	4.40	6.47 ± 0.05	3.20 ± 0.05	27.04 ± 0.20	0.387 ± 0.006					
14	5.05	2	Al, 2.0	4.20	6.81 ± 0.05	3.49 ± 0.05	31.04 ± 0.20	0.373 ± 0.006					

Table 1. Parameters and results of the experiments when determining the shock compressibility of ballistic Kevlar with various orientation of the fibers

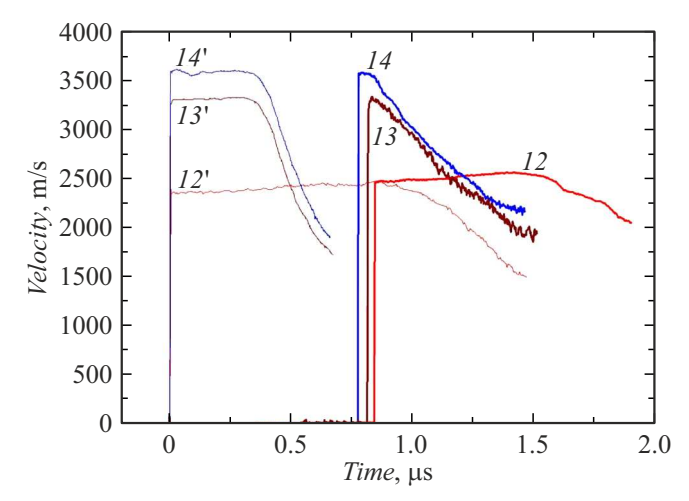


Figure 6. Particle velocity profiles at the sample/water interface with longitudinal orientation of the fibers and the pressure above 15 GPa.

7, 13 and 14, the thickness of the projectiles was 2 mm, so the time of existence of the constant values of the velocity behind the shock wave in the entering pulse is $0.3 \,\mu s$. With propagation through the sample, this time is reduced and to the time of exit to the boundary with water it does not exceed $0.1 \,\mu s$. So, the dependences 6, 7 (Fig. 4) and 13, 14 (Fig. 6) have an unnoticeable area of the constant values

of the parameters and a velocity drop is observed almost immediately behind a shock jump. It should be noted that despite a heterogeneous structure of the studied samples the velocity profiles are quite smooth.

The most pronounced feature of the velocity profiles in the samples with longitudinal orientation of the fibers in relation to the direction of propagation of the shock wave is the two-wave configuration at the pressure of shock compression below 12 GPa (Fig. 5). In this case, unlike transverse orientation (Fig. 3), the first wave, whose amplitude of about 60 m/s, first reaches the interface with the window. The velocity of its propagation within the measurement error coincides with the speed of sound in the longitudinal direction of the fibers $C_{\parallel} = 5.30 \, \mathrm{km/s}$. This result complies with the previous papers which have studied the structure of the wave profiles in the composites when the shock waves propagate along the fibers [5,12,13,39,42]. The second main wave of shock compression propagates with the lesser velocity U_s . The time of arrival of this wave to the boundary with the window is determined by its amplitude and the sample thickness. At the pressure of approximately 12.6 GPa, the velocity of the second wave reaches the value that coincides with C_{\parallel} , and the twowave configuration disappears. At the same time, the shock wave becomes a single one (the tests 12–14). Since the precursor amplitude is small as compared to the maximum value of the velocity in the second wave, its presence does

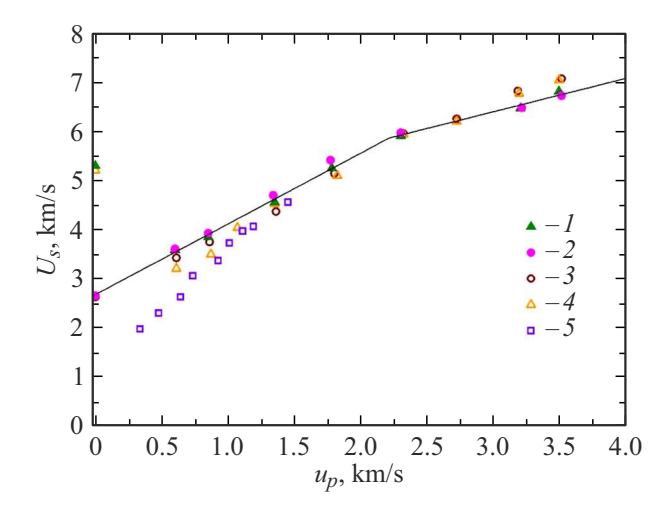


Figure 7. Shock Hugoniot of ballistic Kevlar with various orientation of the fibers: the filled circles — transverse orientation; the filled triangles — longitudinal orientation: 1, 2 — the present paper; 3, 4 — the paper [5], 5 — the paper [3]. The solid lines — approximation of the experimental data.

not result in significant distortion of the velocity profiles that are almost the same for both orientations of the fibers.

Processing of the experimental data resulted in plotting the shock Hugoniot for the samples of ballistic Kevlar with the epoxy resin with different orientation of the fibers in relation to the direction of propagation of the shock wave. The results are shown on Fig. 7 in the coordinates the shock wave velocity U_s — the particle velocity u_p . Besides, for comparison there are experimental data for the composites based on Kevlar with the epoxy matrix [5] and the phenol matrix [3]. The filled circles correspond to transverse orientation, while the filled triangles correspond to longitudinal The discrepancy of the results obtained for different orientation of the fibers insignificantly exceeds the error of the experiments, therefore, it can be assumed that the shock compressibility of ballistic Kevlar does not depend on the direction of propagation of the shock waves. With the particle velocity of 2.2 km/s, which approximately corresponds to 17 GPa, the dependence $U_s(u_p)$ exhibits a clear break that corresponds to a start of chemical destruction in the composite. When $u_p < 2.2 \,\mathrm{km/s}$, the shock Hugoniot is well approximated by the linear $U_s(u_p)$ relationship

$$U_s = 2.68 + 1.44 \cdot u_p$$
, [km/s],

wherein, the first coefficient with good accuracy coincides with the measured speed of sound $C_{\perp}=2.66\,\mathrm{km/s}$ for transverse orientation of the fibers. Above the break area, increase of the shock wave velocity on the particle velocity slows down. At this, when $u_p>2.2\,\mathrm{km/s}$ the shock Hugoniot can also be described by the linear $U_s(u_p)$ relationship

$$U_s = 4.25 + 0.70 \cdot u_p$$
, [km/s].

Chemical destruction of the polymer under shock-wave impact results in origination of specific features on the shock Hugoniots and is considered, for example, in the paper [43].

3. Spall strength of the composite based on ballistic Kevlar

The strength of the samples that consist of ballistic Kevlar and the epoxy resin under pulse tension was determined in the conditions of spall fracture when the compression pulses are reflected from the free surface of the material [41]. Interaction of incident and reflected rarefaction waves inside the sample results in tensile stresses that can lead to The present study has used a method of its fracture. measurement of resistance of the materials to spall fracture, which is based on recording the velocity of the free surface of the sample. Fig. 8 shows a nature of the velocity change in case of spallation. Exit of the shock wave to the free surface causes abrupt increase of the surface velocity to the maximum value W_m . The dashed line marks variation of the velocity without fracture. Exit of the compression wave formed as a result of spallation to the free surface results in increase of the velocity and origination of the socalled spall pulse. In Fig. 8, this time is designated by t_s marked with a vertical arrow. The respective velocity value is equal to W_s . Analysis of the process of interaction of the incident and reflected rarefaction waves by a characteristics method provides a relationship between a stress in the spall plane σ_s and a value of drop of the velocity of the free surface $W_m - W_s$ [44]:

$$\sigma_{s} = 0.5\rho_{0}C_{0}(W_{m} - W_{s}), \tag{1}$$

where ρ_0 , C_0 are, respectively, the density of the material and the volume speed of sound in it, which coincides with C_{\perp} . The relationship (1) is true for a medium that has not

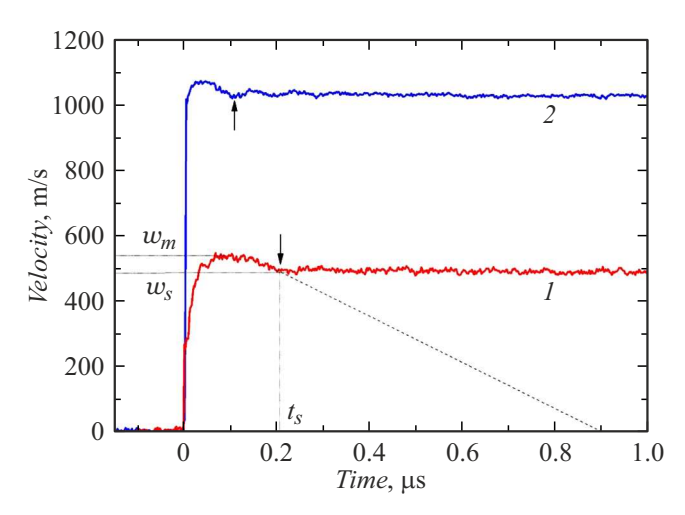


Figure 8. Velocity profiles of the free surface of ballistic Kevlar with transverse orientation of the fibers. The vertical arrows mark the time of exit of the spall pulse to the free surface.

Nº	W_i , m/s h_i , mm		h_b , mm	h_s , mm	ΔW , m/s	σ_s , MPa						
Transverse orientation of the fibers												
1	650	0.4	PMMA, 2	2.97	58 ± 1	100 ± 1						
2	650	2	PMMA, 2	4.35	50 ± 1	87 ± 1						
Longitudinal orientation of the fibers												
3	650	0.4	PMMA, 2	4.30	91 ± 1	158 ± 1						
4	650	2	Cu, 2	4.40	$28/82 \pm 1$	$48/142 \pm 1$						
5	650	2	PMMA, 2	4.45	104 ± 1	180 ± 1						

Table 2. Parameters and results of the experiments when determining the spall strength of ballistic Kevlar with various orientation of the fibers

elastic-plastic properties and usually used for determining the spall strength of the composites [31].

The results of determination of the spall strength and the parameters of the experimental assemblies are given in Table 2. The designations of the magnitudes are the same as in Table 1. The measured velocity profiles of the free surface are shown on the figures 8, 9. The digit designations of the profiles of the figures correspond to a test number of Table 2. The time of exit of the spall pulse to the free surface is marked with the vertical arrow. Fig. 8 shows results for Kevlar with transverse orientation of the fiber with two different pressures of shock compression. At this, the value of the spall strength varies insignificantly and does not exceed 100 MPa. The profile 2 has a quite clear spall pulse and exhibits subsequent velocity oscillations due to waves reverberation in a spall plate. Dissipative losses result in fast attenuation of these oscillations and establishment of a constant velocity of motion of the spall plate. Intensity of dissipation increases with decrease of the pressure of shock compression and the profile 1 has an almost constant velocity after a weakly pronounced spall pulse.

Fig. 9 show the velocity profiles of the free surface for longitudinal orientation of the fibers. In this case, with exit of the compression pulse to the free surface, a two-wave configuration is recorded. The amplitude of the first wave exceeds the values mentioned in the previous section and reaches the value of 100 m/s, which is due to unloading into air instead of water. The test 5 recorded the velocities of the free surface of the sample in two points: in a central part of the sample (a brown profile) and at the distance of 10 mm from the center(a pink profile), which was a half distance from the center to a lateral surface. Lateral unloading insignificantly reduces the amplitude of the compression pulse, but the value of the spall strength is the same and is equal to 180 MPa. The deceleration of the spall plate is noticeable, the velocity of which decreases approximately by 50 m/s in a few microseconds.

In the test 4, the spall fracture of the sample is much unclearer than, for example, in the test 5, and it is almost impossible to distinguish the spall pulse on the velocity

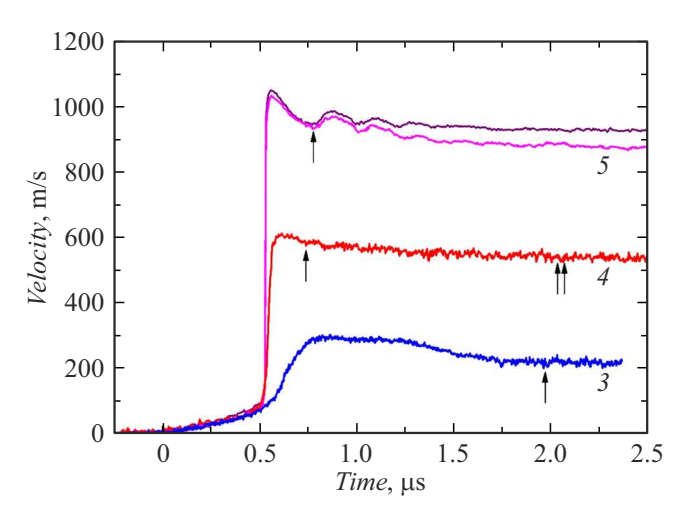


Figure 9. Velocity profiles of the free surface of the studied composite with parallel orientation of the fibers. The vertical arrows mark the time of exit of the spall pulse to the free surface.

profile of the free surface. The single vertical arrow marks the time after which the recorded velocity profile is overestimated in relation to the initial pulse. In this case, the respective value of the tensile stresses is a threshold of start of fracture, which is 28 MPa and designated by the first digit in Table 2. After fracture start, the velocity of the free surface continues to decrease and this indicates that after fracture start the spall plate is not separate from the bulk of the sample. At the same time, the tensile stresses in the spall plane continue to rise. The double vertical arrow marks the time, after which there is no noticeable drop of the velocity and it is this value that is assumed to be equal to W_s . In this case, the value of the spall strength can be determined only approximately, since it depends on kinetics of spall fracture, as demonstrated by authors of the paper [45]. In particular, it is noted in the paper [45] that with the constant fracture rate it is possible to use the above-mentioned calculation relationship (1) for determining σ_s . It gives the value of 82 MPa for the magnitude of the spall strength, which is

provided in Table 2 by the second digit. The similar nature of the change of free surface velocity is observed in the test 3, too, which is without the spall pulse as well. In this case, the vertical arrow marks the time, after which the velocity remains constant.

Conclusion

The obtained particle velocity profiles for the samples made of ballistic Kevlar in the epoxy matrix exhibit a number of the specific features related to a heterogeneous structure of the studied material — with longitudinal orientation of the fibers in relation to the direction of propagation of the shock wave, the two-wave structure is formed. As in other similar anisotropic composites [5,9,39], it is realized under certain pressures of shock compression, when U_s is less than a speed of propagation of disturbances along the fibers This range of the pressures depends on the value of the speed of sound along the fibers. For example, in carbon fiber-reinforced plastic, due to higher values of the speed of sound in the carbon fibers and the density of the material, the two-wave configuration can be observed up to the pressures of about 30 GPa [39,42], wheres both in the Kevlar samples [5] and the studies samples based on ballistic Kevlar it is only recorded at up to 12.2 GPa. When the velocity of the second shock wave becomes comparable to or higher than the speed of sound in the longitudinal direction, a single shock wave propagates in the samples in the same way as with transverse orientation of the fibers.

It should be noted that the particle velocity profiles do not exhibit any specific features that would indicate chemical decomposition of Kevlar. Thus, for example, the dependences 5 and 12 of the figures 4 and 6 demonstrate a wave profile that is typical for media, in which there is no chemical transformation under shock-wave impact. At the same time, as previously noted, in the epoxy resin that is a binder component of this composite chemical destruction around 20 GPa results in increase of the velocity behind the shock jump for several tens of nanoseconds [23]. Presence of the aramid fibers results in disappearance of this specific feature.

By comparing the experimental dependences of the shock wave velocity U_s on the particle velocity u_p (Fig. 7) for the composites based on Kevlar with a different type of the matrices — the epoxy matrix [5] and the phenol matrix [3] — it can be noted that there is a good match between the provided data within the studied range of the velocities. Probably, a small difference is caused by the internal structure of specific sample, which is most vividly manifested at the low pressures. Chemical destruction in the Kevlar samples [5] and in the studied samples based on ballistic Kevlar, which is manifested as the break on the dependence $U_s(u_p)$, begins at the same values of the particle velocity $u_p = 2.2 \, \mathrm{km/s}$.

It is clear from Table 2 that the value of the spall strength of the studied composite depends on orientation

of the fibers. The maximum values of σ_s are realized with longitudinal orientation of the fibers and do not exceed about 180 MPa, which is almost in two times less than the strength of the epoxy resin [22,24,26] that is used as the binder component. It indicates that in conditions of shockwave impact fracture occurs along the fiber/matrix interface. It should be noted at the same time that in the composite with the similar composition and the similar structure [5], the value of the spall strength for the two orientations of the fibers is virtually independent of the direction of propagation of the shock wave through the material. Probably, the samples of the present study and the article [5] exhibit different adhesion between the aramid fabric layers and the epoxy binder. Since its value is usually small due to low surface energy of the aramid fiber, some manufacturers modify the fiber surface, which in turn can affect the value of the spall strength σ_s of the obtained composite. Thus, it is clear from the performed experiments that despite the similar composition and the similar structures of the samples, each case exhibits the individually pronounced response of the materials to the pulse impact.

Funding

The study has been performed in accordance with the State assignment subject N_2 124020600049-8.

Conflict of interest

The authors declare that they have no conflict of interest.

References

- [1] S. Katz, E. Grossman, I. Gouzman, M. Murat, E. Wiesel, H.D. Wagner. Int. J. Impact Eng., 35 1606 (2008).
- [2] D.M. Dattelbaum, J.D. Coe, P.A. Rigg, R.J. Scharff, J.T. Gammel. J. Appl. Phys., 116, 194308 (2014).DOI: 10.1063/1.4898313
- [3] T. Homae, T. Shimizu, K. Fukasawa, O. Masamura. J. Reinf. Plast. Compos., 25, 1215 (2006).DOI: 10.1177/0731684406066370
- [4] A.V. Bushman, V.P. Efremov, V.E. Fortov, G.I. Kanel,
 I.V. Lomonosov, V.Y. Ternovoi, A.V. Utkin. Matter, 1991, 79 (1992). DOI: 10.1016/B978-0-444-89732-9.50018-2
- V. Mochalova, A. Utkin, A. Savinykh, G. Garkushin. Compos. Struct., 273, 114309 (2021).
 DOI: 10.1016/j.compstruct.2021.114309
- [6] D.M. Dattelbaum, J.D. Coe. The dynamic-loading response of carbon-fibre-filled polymer composites. In: Dyn. Deform. Damage Fract. Compos. Mater. Struct. (Elsevier, 2023), p. 195–244.
- [7] J.C.F. Millett, N.K. Bourne, Y.J.E. Meziere, R. Vignjevic, A. Lukyanov. Compos. Sci. Technol., 67, 3253 (2007). DOI: 10.1016/j.compscitech.2007.03.034
- [8] W. Riedel, H. Nahme, K. Thoma. Equation of state properties of modern composite materials: Modeling shock, release and spallation, In: AIP Conf. Proc. (American Institute of Physics, 2004), p. 701–706. DOI: 10.1063/1.1780335

- [9] C.S. Alexander, C.T. Key, S.C. Schumacher. J. Appl. Phys., 114, 223515 (2013). https://doi.org/10.1063/1.4846116.
- [10] S.A. Bordzilovskii, S.M. Karakhanov, L.A. Merzhievskii. FGV, (in Russian). **33**, 132 (1997).
- [11] A.V. Bushman, V.P. Efremov, I.V. Lomonosov, A.V. Utkin, V.E. Fortov. TVT, 28, 1232 (1990) (in Russian).
- [12] V.M. Mochalova, A.V. Utkin, V.E. Rykova, M. Endres, D.H.H. Hoffmann. Arch. Mech., 71, 417 (2019). DOI: 10.24423/aom.3144
- [13] T. Lässig, F. Bagusat, S. Pfändler, M. Gulde, D. Heunoske, J. Osterholz, W. Stein, H. Nahme, M. May. Struct., 182, 590 (182). DOI: 10.1016/j.compstruct.2017.09.031
- [14] S. Khatiwada, C.A. Armada, E.V. Barrera. Procedia Eng., 58, 4 (2013).
- [15] C. Frias, S.A. Macdonald, D. Townsend, N.K. Bourne, C. Soutis, P.J. Withers. 19th Biennial Conference of the APS Topical Group on Shock Compression of Condensed Matter, Florida, 60 (8), M1–056 (2015).
- [16] S. Yang, V.B. Chalivendra, Y.K. Kim. Compos. Struct., 168, 120 (2017).
- [17] I. Taraghi, A. Fereidoon, F. Taheri-Behrooz. Mater. Des., 53, 152 (2014). DOI: 10.1016/j.matdes.2013.06.051
- [18] P.N.B. Reis, J.A.M. Ferreira, Z.Y. Zhang, T. Benameur, M.O.W. Richardson. Compos. Part B Eng., 46, 7 (2013). DOI: 10.1016/j.compositesb.2012.10.028
- [19] W. Xie, W. Zhang, L. Guo, Y. Gao, D. Li, X. Jiang. Compos. Part B Eng., 153, 176 (2018).
- [20] C. Pirvu, L. Deleanu, C. Lazaroaie. Ballistic tests on packs made of stratified aramid fabrics LFT SB1. In: IOP Conf. Ser. Mater. Sci. Eng., IOP Publishing, 2016: p. 012099. https://iopscience.iop.org/article/10.1088/1757-899X/147/1/012099/meta (accessed October 3, 2024).
- [21] M.J. Donough, B.G. Prusty, M.J. Van Donselaar, E.V. Morozov, H. Wang, P.J. Hazell, A.W. Philips, N.A. St John. Int. J. Impact Eng., 171, 104373 (2023).
- [22] V. Mochalova, A. Utkin, A.V. Pavlenko, S.N. Malyugina, S.S. Mokrushin. ZhTF, 89, 126 (2019) (in Russian).
- [23] V. Mochalova, A. Utkin, D. Nikolaev, A. Savinykh, G. Garkushin, A. Kapasharov, G. Malkov. J. Appl. Phys., 136, 045902 (2024). DOI: 10.1063/5.0217287
- [24] A.E. Tarasov, E.R. Badamshina, D.V. Anokhin, S.V. Razorenov, G.S. Vakorina. ZhTF, 88, 34 (2018) (in Russian).
- [25] T.A. Rostilov, V.S. Ziborov. TVT, 60, 922 (2022) (in Russian).
- [26] J.E. Pepper, J. Huneault, M. Rahmat, B. Ashrafi, O.E. Petel. Int. J. Impact Eng., 113, 203 (2018).
- [27] J. Huneault, J.E. Pepper, M. Rahmat, B. Ashrafi, O.E. Petel.
 J. Dyn. Behav. Mater., 5, 13 (2019).
 DOI: 10.1007/s40870-018-00180-w
- [28] R.C. Huber, J. Peterson, J.D. Coe, D.M. Dattelbaum, L.L. Gibson, R.L. Gustavsen, J.M. Lang, S.A. Sheffield. J. Appl. Phys., 127, 105902 (2020). DOI: 10.1063/1.5124252
- [29] R.C. Huber, D.M. Dattelbaum, J.M. Lang, J.D. Coe, J.H. Peterson, B. Bartram, L.L. Gibson. J. Appl. Phys., 133, 035106 (2023).
- [30] P.J. Hazell, H. Wang. Shock response of polymer composites. In: Dyn. Deform. Damage Fract. Compos. Mater. Struct. (Elsevier, 2023), p. 309–336. https://www.sciencedirect.com/science/article/pii/B9780128239797000120 (accessed April 10, 2024)
- [31] F. Yuan, L. Tsai, V. Prakash, A.M. Rajendran, D.P. Dandekar. Int. J. Solids Struct., 44, (2007) 7731 (2007).

- [32] E. Zaretsky, G. DeBotton, M. Perl. Int. J. Solids Struct., 41, 569 (2004). DOI: 10.1016/j.ijsolstr.2003.09.026
- [33] A.V. Utkin, V.M. Mochalova, V.V. Yakushev, V.E. Rykova, M.Yu. Shakula, A.V. Ostrik, V.V. Kim, I.V. Lomonosov. TVT, 59, 189 (2021) (in Russian). DOI: 10.31857/S0040364421020137
- [34] A.V. Utkin. PMTF, 34, 140 (1993) (in Russian).
- [35] A.V. Fedorov, A.L. Mikhailov, S.A. Finyushin, D.A. Kalashnikov, E.A. Chudakov, E.I. Butusov, I.S. Gnutov. ZhETF, 149, 792 (2016) (in Russian).
- [36] N.Kh. Akhmadeev, G.M. Gainatulina. Pis'ma v ZhTF, 11, 897 (1985) (in Russian).
- [37] D.C. Wood, G.J. Appleby-Thomas, A. Hameed, N.R. Barnes, A. Hughes, P.J. Hazell. J. Mater. Sci., 53, 11415 (2018). DOI: 10.1007/s10853-018-2431-0
- [38] P.-L. Hereil, O. Allix, M. Gratton. J. Phys., IV (7), C3 (1997). DOI: 10.1051/jp4:1997391
- [39] V. Mochalova, A. Utkin, D. Nikolaev. J. Appl. Phys., 133, 240701 (2023). DOI: 10.1063/5.0151292
- [40] A.P. Kuznetsov, S.A. Kolesnikov, A.A. Golubev, K.L. Gubskii, S.V. Dudin, A.V. Kantsyrev, V.I. Turtikov, A.V. Utkin, V.V. Yakushev. PTE, (in Russian). 3, 116 (2011).
- [41] G.I. Kanel', S.V. Razorenov, A.V. Utkin, V.E. Fortov. *Udarno-volnovye yavleniya v kondensirovannykh sredakh* (Yanus-K, M., 1996) (in Russian).
- [42] V. Mochalova, A. Utkin, V. Sosikov, V. Yakushev, A. Zhukov. Shock Waves, 32, 715 (2022). https://doi.org/10.1007/s00193-022-01104-3.
- [43] D.M. Dattelbaum, J.D. Coe. Polymers, 11, 493 (2019).DOI: 10.3390/polym11030493
- [44] S.A. Novikov, I.I. Divnov, A.G. Ivanov. Fizika metallov i metallovedenie, 21, 608 (1966) (in Russian).
- [45] A.V. Utkin, V.A. Sosikov. PMTF, 46, 29 (2005) (in Russian).

Translated by M.Shevelev